Journal of Modern Optics
Publication details, including instructions for authors and subscription information:
http://www.informaworld.com/smpp/title~content=t713191304

Focusing on factorability: space-time coupling in the generation of pure heralded single photons

Peter J. Mosley [a]; Jeff S. Lundeen [a]; Brian J. Smith [a]; Ian A. Walmsley [a]
[a] Clarendon Laboratory, University of Oxford, Oxford, UK

First Published:January2009

To cite this Article Mosley, Peter J., Lundeen, Jeff S., Smith, Brian J. and Walmsley, Ian A.(2009)'Focusing on factorability: space-time coupling in the generation of pure heralded single photons',Journal of Modern Optics,56:2,179 — 189
To link to this Article: DOI: 10.1080/09500340802187324
URL: http://dx.doi.org/10.1080/09500340802187324

Journal of Modern Optics
Vol. 56, Nos. 2–3, 20 January–10 February 2009, 179–189

Taylor & Francis
Taylor & Francis Group

Focusing on factorability: space–time coupling in the generation of pure heralded single photons

Peter J. Mosley[a]*, Jeff S. Lundeen[a], Brian J. Smith[a] and Ian A. Walmsley[a]

Clarendon Laboratory, University of Oxford, Oxford, UK

(*Received 31 January 2008; final version received 6 May 2008*)

The interference of single heralded photons from multiple parametric downconversion sources requires photon pairs in factorable states. Typically, these are selected from an ensemble of pairs by narrow filters that remove any exhibiting correlations. In order to eliminate these lossy filters, factorable photon pairs free from any spatio-temporal correlations must be created directly at each source. This requires careful engineering of the group velocity dispersion of the nonlinear crystal in which pair generation takes place. Several schemes have been proposed to do this in the plane-wave regime, but in a realistic experiment one must also take into account the effects of focusing on the two-photon state. Focusing leads to space–time coupling between the pump structure and the downconverted pairs that has the potential to reduce their factorability, but if carefully managed can actually increase it. In this paper, we consider some of the effects of focusing and their consequences for pure single photon generation.

Keywords: photon; parametric downconversion; pure state; heralding

1. Introduction

During the last two decades, the generation of photon pairs by parametric downconversion (PDC) has been the mainstay of quantum optics laboratories [1,2]. The ability to conditionally prepare a single photon on the detection of its twin using only a pump laser, a nonlinear crystal or two, and some filters has facilitated a plethora of experiments from fundamental tests of quantum mechanics [3,4] to demonstrations of photonic quantum information processing (QIP) protocols [5,6].

However, when used as heralded sources of single photons, standard downconverters have a significant drawback. The pair generation process is constrained by energy and momentum conservation with a degree of strictness dependent on the pump bandwidth and crystal length, respectively. These restrictions lead to strong correlations between the degrees of freedom of each daughter photon and those of its twin. Measuring the herald photon with a detector unable to resolve these parameters then projects the remaining photon into a mixed state, something that is undesirable for QIP schemes. This process is most easily explained by considering the Schmidt decomposition of the joint two photon state [7] – the reduction in the purity of the heralded photon is related to the number of Schmidt modes present initially. In this article, we discuss correlation in the frequency–time degrees of freedom; spatial correlations can be eliminated by careful focusing to obtain preferential emission into a single spatial mode and coupling the downconversion into single mode fibres to remove any other unwanted modes.

Several experiments have successfully interfered heralded single photons prepared in separate sources despite strong frequency correlations within the pairs [8–10]. This was made possible by placing narrow spectral filters in the path of one or both of the daughter photons. These filters select only those pairs that do not exhibit spectral correlations and discard the remainder, so that, when detecting one photon as a herald, its twin remains in a pure state. There are several significant drawbacks to this technique. The purity of the single photon only approaches unity as the filter bandwidth tends to zero, so perfect purity is only achieved when no photons are transmitted through the filters. The need for very narrow filters inevitably introduces a high level of loss to the system and, in the case where both downconversion arms are filtered, the heralding efficiency will therefore be very low. This loss presents a serious problem if one wishes to conduct experiments involving several pairs of photons: for a filter with a transmission probability of 25% for each photon, the likelihood of one pair passing the filter is only 6%, and the probability of having two pairs present after filtering (given that two pairs were generated in the first place, itself an unlikely event) is only 0.4%. This approach is clearly not

*Corresponding author. Email: p.mosley1@physics.ox.ac.uk

ISSN 0950–0340 print/ISSN 1362–3044 online

DOI: 10.1080/09500340802187324
http://www.informaworld.com

scalable to the production of quantum states with high photon number. Furthermore, any loss in the system quickly degrades entanglement in photon number, a property that is vital for continuous-variable entanglement distillation protocols.

2. Pure single photon generation in the plane-wave regime

An alternative to generating numerous photon pairs and discarding most of them by filtering is to prepare photon pairs directly in factorable states so that unwanted correlations do not exist in the first place. Several proposals have been published for the control of spectral correlations in PDC sources based on engineering the pump beam, the nonlinear crystal, or the relationship between the two. In this paper we concentrate on a factorable state generation technique based on the group velocity dispersion characteristics of particular nonlinear crystals aided by the flexibility offered by a broadband ultrafast pump pulse.

By considering the first-order Taylor expansion of the phase mismatch between plane-wave pump and downconverted photons in a nonlinear crystal, in 2001 Grice et al. discovered that by satisfying certain conditions on the group velocities of the three fields, and providing that the bandwidth of the pump was sufficiently broad, spectrally decorrelated photon pairs could be created [11]. One desirable regime was found to occur where the group velocity of one daughter photon matches that of the pump pulse. This is possible for particular sets of wavelengths in all common birefringent nonlinear crystals through type-II phasematching in which the pump decays into two photons in orthogonally polarised modes. It can be arranged that, as a result of the birefringence, the photon polarised perpendicular to the pump is group velocity matched to it. The downconverted photon polarised in the same plane as the pump inevitably travels at a different group velocity and so this arrangement became known as 'asymmetric' group velocity matching.

The state from a downconverter up to the two-photon contribution can be represented as a vacuum term plus the product of a pump envelope function, $\alpha(\omega_s+\omega_i)$, with the phasematching function of the crystal, $\phi(\omega_s,\omega_i)$:

$$|\Psi(\omega_s,\omega_i)\rangle = |0\rangle + \eta\iint \mathrm{d}\omega_s\,\mathrm{d}\omega_i \alpha(\omega_s+\omega_i)\phi(\omega_s,\omega_i) \times a_e^\dagger(\omega_s)a_o^\dagger(\omega_i)|0\rangle \quad (1)$$

$$= |0\rangle + \eta\iint \mathrm{d}\omega_s\,\mathrm{d}\omega_i f(\omega_s,\omega_i)a_e^\dagger(\omega_s) \times a_o^\dagger(\omega_i)|0\rangle. \quad (2)$$

The probability of creating a pair is $|\eta|^2$, $a_e^\dagger(\omega_s)$ and $a_o^\dagger(\omega_i)$ are the creation operators for photons in polarisation modes e and o, and we have considered explicitly only the frequencies, ω_s and ω_i, of the two photons. $f(\omega_s,\omega_i)$ is the joint spectral amplitude of the two-photon state. The pump envelope function ensures energy conservation between the three fields in the process of downconversion. The function is a Gaussian envelope centered on the line $\omega_p=\omega_s+\omega_i$:

$$\alpha(\omega_s+\omega_i) = \exp\left[-\left(\frac{\omega_s+\omega_i-2\omega_0}{\sigma}\right)^2\right]. \quad (3)$$

The phasematching function is centered on the line of momentum conservation and has the standard sinc function form:

$$\phi(\omega_s,\omega_i) = \exp\left[\frac{\mathrm{i}(k_s+k_i-k_p)L}{2}\right]\mathrm{sinc}\left[\frac{(k_s+k_i-k_p)L}{2}\right], \quad (4)$$

where for the collinear case all nonzero wavevectors are in the longitudinal direction. The case in which we are interested is the type-II phasematching function for a nonlinear crystal a few millimetres in length where the wavelengths of the interacting fields are such that one daughter photon travels at the same group velocity as the pump. The function is broadband in the frequency of the velocity-matched photon but narrow in the other, and the frequency of one photon has no dependence on that of its twin. When multiplied by a broadband pump function, it is principally the phasematching function that shapes the overall two-photon state. The resulting joint probability amplitude can then be factorised into a function of the signal photon frequency multiplied by a function of the idler frequency: $f(\omega_s,\omega_i)=g(\omega_s)h(\omega_i)$. This is a direct result of asymmetric group velocity matching.

As well as bulk PDC sources, asymmetric group velocity matching can be applied to a variety of other media to generate factorable photon pairs. In their paper from 2006, U'Ren et al. showed that a sequence of bulk nonlinear crystals separated by appropriate lengths of birefringent material (so-called 'superlattices') could produce photon pairs with an arbitrary degree of frequency correlation, including no correlations at all [12]. These constructions work by achieving effective group velocity matching between the mean velocities of the pump and one daughter photon. The birefringent spacers are orientated such that the temporal walkoff between the relevant downconverted photon and the pump has the opposite value to that in the nonlinear segments. This method is very flexible as one can design the structure to suit any requirements, however it has the practical drawback that the

individual components must be manufactured with very strict thickness tolerances.

Another system in which group velocity matching can be exploited is pair generation by spontaneous four-wave mixing in fibre. By choosing the pump wavelength such that one of the degenerate photons in each pair is group velocity matched to the pump, factorable state generation is assured. However, for a typical fibre the frequency of one of the photons will probably not be within an acceptable range given current detector technology. Instead, by using a photonic crystal fibre (PCF) with a custom designed core diameter and air fill fraction, one can engineer the dispersion characteristics to allow factorable pair generation at a more advantageous pair of wavelengths. This was recently investigated theoretically by Garay-Palmett et al. [13], though the relative difficulty of obtaining custom-drawn PCF has hindered experimental progress.

The nonlinear crystal selected for the experiments presented in this paper was potassium dihydrogen phosphate (KDP). The dispersion characteristics of KDP are such that the group velocity matching condition is satisfied at a convenient pair of wavelengths – pumping at 415 nm with a frequency-doubled ultrafast titanium:sapphire oscillator and detecting the downconversion at 830 nm with high-efficiency silicon avalanche photodiodes. As KDP is a negative uniaxial crystal, e-ray pump pulses are group velocity matched with orthogonally-polarised o-ray downconverted photons, while their e-ray twins walk off temporally from the pump.

The joint two-photon state for type-II collinearly phasematched KDP pumped at 415 nm is shown in Figure 1. The factorability of the state, and hence the anticipated purity of the heralded photons, can be found straightforwardly from the numerical analogue of the Schmidt decomposition – the singular value

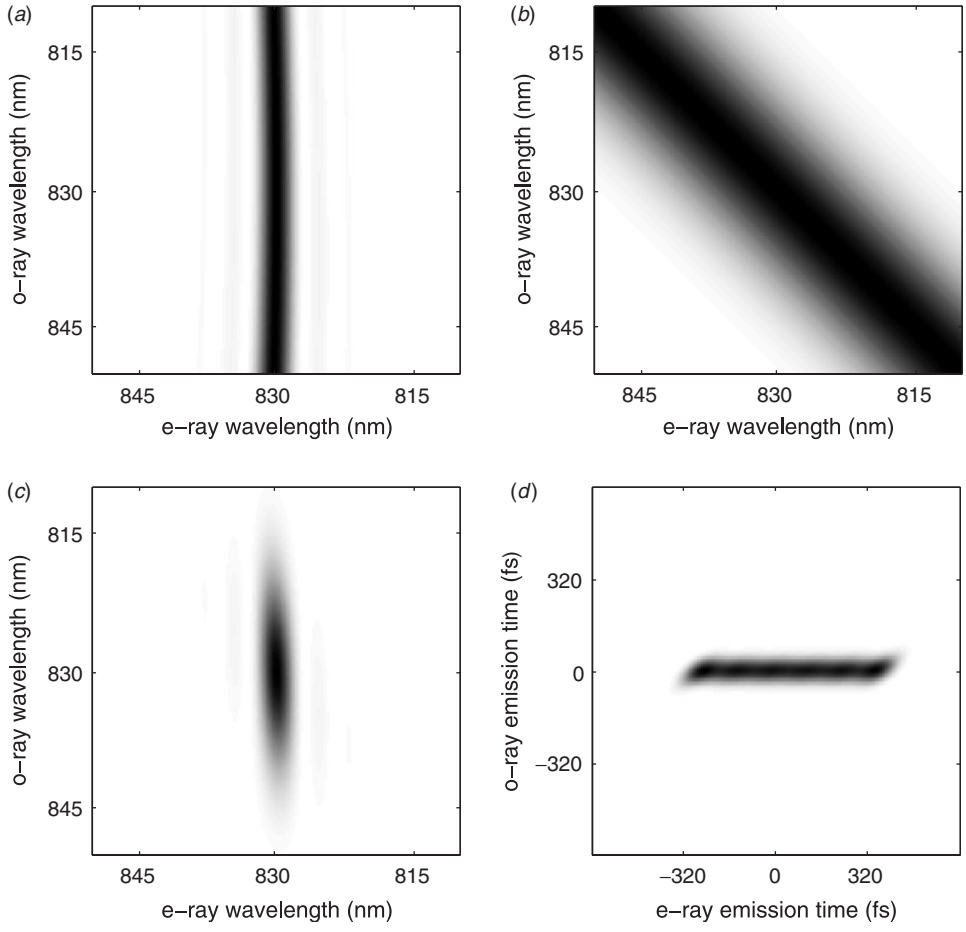

Figure 1. Type-II collinear phasematching function (*a*) for a 5 mm KDP crystal centered at 830 nm. Gaussian pump function (*b*) for ultrafast pulses with mean wavelength of 415 nm and a spectral bandwidth of 4 nm FWHM. Resulting joint spectral intensity (*c*) demonstrating almost no correlation between signal and idler frequencies. The corresponding joint temporal intensity (*d*) also shows minimal correlations between the emission times as a result of the flat phase across the joint spectral amplitude.

decomposition (SVD) of the joint amplitude. The purity of either reduced state is simply the sum of the squares of the singular values [14]. For a 5 mm long KDP crystal and a pump bandwidth of 4 nm full width at half maximum (FWHM), the maximum achievable purity is 0.953.

It is not immediately obvious how the asymmetric group velocity matching condition physically leads to a factorable joint state. The most intuitive explanation is to consider the temporal picture of the interaction. As the pump pulse travels through the crystal, the amplitude for the emission of an o-ray photon keeps pace with the pump pulse and any o-ray downconversion is automatically generated in the same narrow single temporal mode as the pump pulse. Therefore, when a pump photon decays into a pair, as the o-ray photon is emitted into a single temporal mode so too is the e-ray. This emission into a single joint temporal mode ensures that the pair is also produced in a single spectral mode and therefore no correlations exist between the frequencies of the daughter photons.

3. Space–time effects

The proposals for factorable state generation outlined in the previous section all assumed that the pump and photon pairs propagated as collinear plane waves. This is the simplest case to consider as only one dimension must be included in the calculation of the final state. This is clearly unphysical in the case of pair generation in a bulk crystal – a more realistic model requires the inclusion of the transverse degrees of freedom of both the photon pairs and the pump. As nonlinear crystals are not centrosymmetric, they inevitably display birefringence. The consequence of the different dispersion properties for light travelling with ordinary and extraordinary polarisations is that the spectral properties of the downconverted photons are coupled to the frequency and transverse momentum of both the pump and their twin.

Several studies have been conducted into the control of frequency correlations by manipulating the spatial structure of the pump and downconverted light. One scheme exploits a side-pumped geometry to generate pairs of counter-propagating photons in a single-mode waveguide [15]. By varying the angle between the pump beam and the waveguide, one can control the spectral properties of the pairs and minimise any correlations in their joint spectrum. This technique has the advantages that it allows a high degree of flexibility in the spectra of the photon pairs as it does not require the nonlinear medium to have specific dispersion properties but has the severe disadvantage that the interaction length between the pump and the medium is so short that the pair generation rate is prohibitively small.

Another method relies on precise control of the relationship between the pump spot size and the length of a bulk nonlinear crystal to generate spectrally factorable photon pairs in strictly defined spatial emission modes from ultrafast pumped type-I PDC [16]. This juxtaposes the negative gradient of the standard type-I longitudinal phasematching function with the positive gradient of the transverse phasematching function to yield a state that is uncorrelated in frequency. The desired relationship between the pump beam diameter and the crystal length can generally be satisfied for any central downconversion wavelength for which phasematching is possible, though the solid angle of the collection apertures must be small limiting the available photon flux.

A third strategy is to engineer the pump beam either by introducing angular dispersion between the spectral components with a diffraction grating [17,18] or by changing the spatial mode with a hologram [19]. The output state from the downconverter can then be imbued with the required properties through the coupling of the spatial and spectral pump characteristics with those of the daughter pairs. Further tuning of the joint state can be performed with additional diffraction gratings in the path of the downconverted light [20]. These approaches are advantageous due to their inherent flexibility but suffer from a limited creation rate of photon pairs due to the depletion of the beams in the shaping processes.

Although none of these methods are used directly here, it is clear that the detailed properties of the pump pulses will have a significant effect on the state of the generated pairs. This is especially important when one considers downconversion with non-zero transverse components. The spatial and spectral characteristics of the pump pulses (and any coupling between the two) are mapped onto the joint state of the downconversion. Furthermore, within a nonlinear crystal the change in refractive index with propagation angle for e-polarised light can have a profound effect on the spectral structure of the photon pairs created. Hence, it is vital to understand the implications of changing either the spectral or spatial parameters of the pump.

4. Implications of focusing

As mentioned previously, the initial proposal for generating spectrally factorable photon pairs presented in Section 2 was calculated entirely for the plane-wave regime, assuming a collimated pump and detection of only the strictly collinear PDC. However, in order

to generate single photons that are in well-defined (preferably single) spatial modes that can easily be distributed to subsequent apparatus in a user-friendly manner, the diverging output from a bulk down-converter must be coupled into single-mode fibre (SMF). To do this efficiently, one must focus the pump into the nonlinear crystal and have optics that collect the PDC over a finite solid angle and couple it into the fibres. To encourage emission into a single spatial mode we set the ratio between the Raleigh range of the pump beam and the crystal length to be a little over one (generally in the range 2–4) [21]. This introduces wavevectors other than the single plane-wave propagation direction considered in Section 2. In the same way that the transverse degrees of freedom can be exploited to bring factorability, as in [16,18,19], the focusing and pump parameters, if not carefully controlled, can be enough to ruin the state factorability. Therefore a successful experiment must be founded upon an understanding of these effects.

4.1. Simple pictures

The first stage of this process is to construct a simple picture that demonstrates the consequences of a focused pump on the joint state through the changes of the pump and phasematching functions. We begin by considering the implications of these two different phenomena upon collinear phasematching in KDP: one is the effect of a varying central pump wavelength and the other is the effect of the crystal anisotropy on the e-ray refractive index as a result of different propagation angles with respect to the crystal's optic axis. This situation is illustrated in Figure 2.

Firstly, varying the central pump frequency $\omega_p = 2\omega_0$ in Equation (3) moves the pump function along the line $\omega_s = \omega_i$. Secondly, the wavevectors in the phasematching function given in Equation (4) are linked to the frequencies of the three fields through the dispersion relations of KDP. For e-ray propagation, the dispersion relationship is dependent on the angle

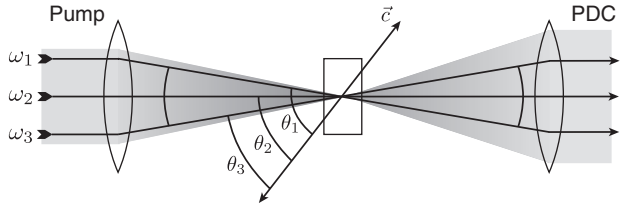

Figure 2. Illustration of collinear phasematching geometry for three different frequencies at at three propagation angles. $\boldsymbol{c}$ is the crystal optic axis. Changing the collinear propagation angle θ_j away from the longitudinal axis is equivalent to propagation along the axis with a rotated crystal.

subtended by the beam and the optic axis and it is for this reason that the phasematching function shifts with changes in the crystal angle relative to the direction of collinear travel [22]. Due to the nontrivial nature of the empirical Sellmeier equations for KDP, the relationship between the phasematched wavelengths and the crystal angle is not simple. However, because the phasematching function is approximately vertical around 830 nm, as the crystal angle changes, the principal transformation of the function is a translation along the narrowband (e-ray) axis. For a constant pump wavelength, this makes the PDC nondegenerate.

These effects are demonstrated in Figure 3 for a 5 mm KDP crystal and an ultrafast pump envelope function with a FWHM bandwidth of 4 nm. The pump functions for three central pump frequencies ω_{1-3} are shown along with the collinear phasematching functions at three crystal angles θ_{1-3}. From these plots it also becomes clear how focusing can lead to spectral correlations in the joint state. Imagine a pump containing three frequency components each of which is focused at a different angle into a KDP crystal. If pump frequency component ω_1 traverses the crystal at phasematching angle θ_1 the joint spectral intensity resulting from this section of the pump beam is shown as the (1, 1) component in part (*c*) of Figure 3. Similarly for pump frequency component ω_2 at angle θ_2 (2, 2) and component ω_3 at angle θ_3 (3, 3). Considering these to be discrete components within a continuous distribution, the collection of the whole output distribution must sum over pump angle. In this case, one can see that the total joint spectrum will remain uncorrelated. However, the case where the direction of frequency change in the pump beam is reversed, we now pair pump frequency component ω_1 with angle θ_3 (1, 3), ω_2 with θ_2 as before (2, 2), and frequency ω_3 with angle θ_1 (3, 1). Rather than compensating for one another as before, the change in pump frequency now compounds the change in phasematching conditions and summing over the output results in a highly correlated state in Figure 3(*d*).

This simple picture demonstrates that one must be very careful with focusing to maintain the factorability of the final joint state. However, the full picture is even more complex as, within the angular distribution of the output, noncollinearly phasematched contributions to the joint state must also be taken into account. A full model of the situation is beyond the scope of this article and will be presented elsewhere.

4.2. Space–time coupling

To couple effectively into SMF, it is inevitable that transverse wavevectors are introduced into both the

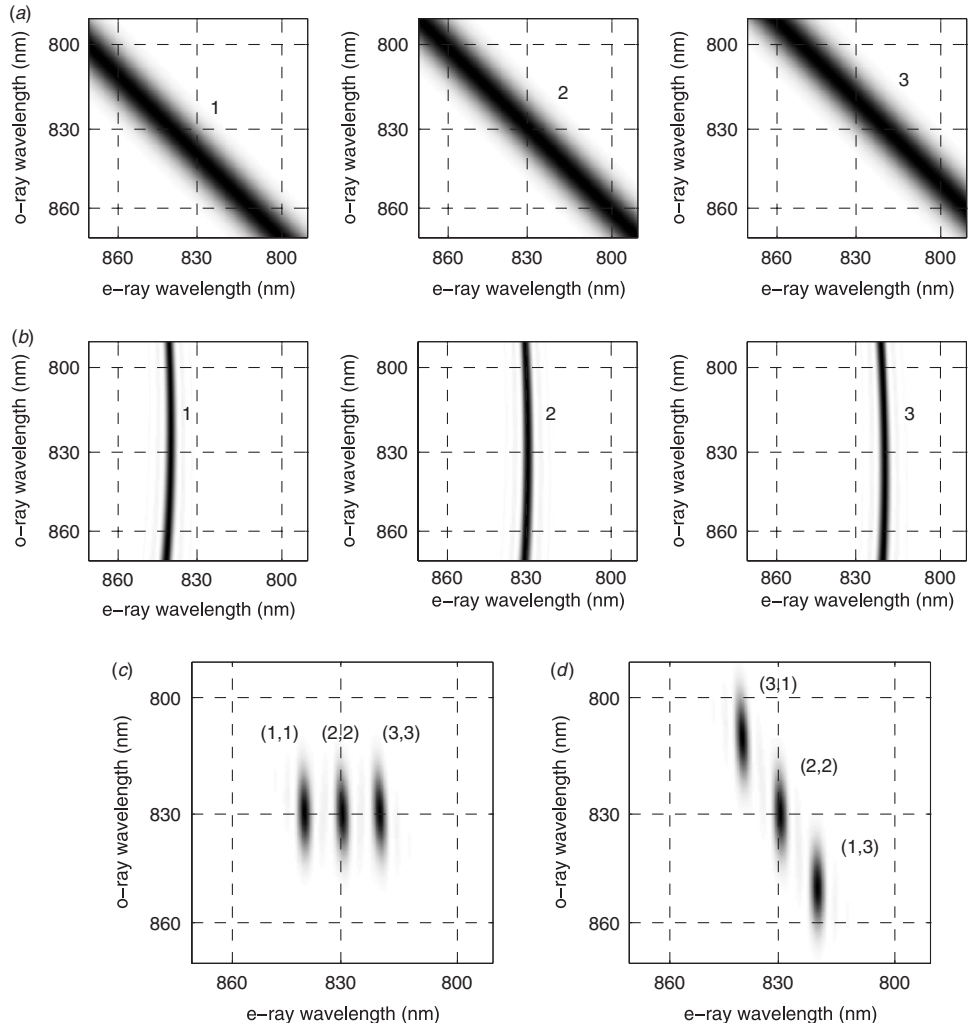

Figure 3. Illustration of how changing the pump frequency and angle of propagation can alter the joint spectrum in the case of a 5 mm KDP crystal and a 4 nm FWHM pump. Three pump functions are shown in (*a*) with central wavelengths separated by 5 nm around 415 nm. Three phasematching functions at different phasematching angles are displayed in (*b*) whose angles differ by 0.5° about 67.8°, the collinear phasematching angle for 830 nm. (*c*) shows the three discrete joint spectra resulting from pairing frequency ω_1 with angle θ_1, ω_2 with θ_2, and ω_3 with θ_3. Summing over this output distribution would result in an uncorrelated state. In (*d*) the functions are paired in the opposite sense: ω_1 with θ_3, ω_2 with θ_2, and ω_3 with θ_1 resulting in a highly correlated total state.

pump and downconverted modes. This complicates the situation (even in the case of a spectrally homogeneous pump) due to the change in phasematching conditions with angle, as described in Section 4.1. The additional wavevectors experience different phasematching conditions and the range of angles acts both to broaden the e-ray frequency distribution and generally increase the level of spectral correlations. What was formerly only a one-dimensional phasematching calculation becomes a three-dimensional one. However, as KDP is a uniaxial crystal it is only necessary to consider two dimensions in the calculation of the joint probability distribution in the focused case; only the projection of the angles of pump and downconverted beams onto the principal plane of the crystal need to be taken into account to obtain a sufficiently accurate result. Yet even in the two-dimensional approximation it is not possible to calculate the level of correlation analytically so it must be found numerically from the SVD of the summed joint distribution.

By summing the noncollinear phasematched output for a range of pump and downconversion angles relative to the optic axis of the crystal a good estimate can be made of the form of the joint state for given experimental parameters, such as the pump focusing, collection angle, crystal length, and pump bandwidth. What becomes clear from this is that, in the case of a transversely homogeneous pump, any focusing inevitably reduces the factorability of the state over that of the plane-wave case. Therefore it would appear

at first sight that the purity of the reduced states from a focused system will be less than that of the idealised strictly collinear case. For typical experimental parameters of focusing a 4 nm FWHM pump with a 250 mm lens and collimating the downconversion from a 5 mm crystal with a 150 mm lens, the purity of the reduced states falls to 0.883.

4.3. Pump spatial chirp

However, another effect must be taken into account when considering focused downconversion. As mentioned earlier, the pump beam is derived from a titanium:sapphire oscillator by frequency doubling in another nonlinear crystal, in this case a 700 μm piece of β-barium-borate (BBO). It is important to make the second harmonic generation (SHG) process as efficient as possible to ensure high count rates from the downconversion, and to do this it is necessary to focus the fundamental titanium:sapphire beam tightly into the SHG crystal. This focusing is much tighter than that used in the PDC crystals and the broad angular distribution results in a large variation in phasematching conditions across the beam. Therefore the wavelength of the second harmonic output is strongly correlated with its direction of emission. After collimation, this becomes a correlation with position – known as spatial chirp. When a spatially chirped pump beam is focused into a PDC crystal, a different central pump wavelength is present at each of the different phasematching angles. This results in a pump function whose central wavelength is correlated with angle subtended with the optic axis of the crystal.

As demonstrated in Figure 3, this can change the level of frequency correlation in the joint state significantly. However, its effects can be predicted by repeating the sum over input and output angles with a central pump frequency that is correlated with angle. The complete joint spectrum can then be seen and the influence of a spatially chirped pump beam found.

5. Harnessing focusing for pure state generation

Although focusing appears at first to be detrimental to the purity of the reduced states, once spatial chirp is included it becomes possible to restore the level of factorability to that of the plane-wave case. Indeed, by carefully balancing the effects of spatial chirp to offset the changing phasematching conditions at different angles, along with the correct choice of pump bandwidth and crystal length, one can engineer a state *more* factorable than the original collinear joint spectrum.

In the majority of nonlinear interactions, such as frequency doubling, it is only the angle of propagation with respect to the optic axis that is the important parameter. However, for a spatially chirped pump beam, the symmetry of phasematching in downconversion is broken and the actual *direction* of the optic axis with respect to the direction of frequency change in the pump beam becomes critical. For a given set of experimental parameters, the difference in the factorability of the final joint state between 'positive' and 'negative' spatial chirp is significant. The reason for this can be explained in terms of the geometry of the phasematching diagrams shown in Figure 3.

For different crystal angles, the e-ray wavelength moves. If the pump function remains stationary, the state resulting from summing over the angular distribution will be correlated as the o-ray wavelength is coupled to the e-ray wavelength by the pump distribution: $\omega_s + \omega_i = \omega_p$. On the other hand, if the pump function changes as the e-ray wavelength shifts, the change in pump function along the 45° line can either exacerbate or nullify the correlation-inducing effects of the variation in phasematching function. This is similar to the two cases shown in Figures 3(*c*) and (*d*). It is the direction of the spatial chirp ('positive' Figure 3(*c*) and 'negative' in Figure 3(*d*)) with respect to the optic axis that dictates whether these two effects sum or cancel and hence it is vital to set the optic axis of the downconversion crystal in the correct direction relative to that of the SHG crystal.

Additionally, the angle over which the output distribution is summed can have a dramatic effect on the overall factorability. If this angle is too large, further correlations may be introduced, whereas if it is too small, the fibre coupling will be poor. Hence, a compromise must be reached for this parameter also. Through careful numerical modelling of the joint spectrum, one can find many combinations of parameters that give good factorability. One of those that coincides with an experimental setup providing good count rates can then be chosen. Plots of two numerically simulated joint spectra are shown in Figure 4 for opposite spatial chirps, demonstrating its influence on the factorability of the joint state.

6. Test of frequency correlation

The final source configuration chosen to yield the best combination of factorability and pair generation rate was a 5 mm KDP crystal with the pump focused by a 250 mm focal length lens and the emission from the crystal collimated by a 150 mm lens placed one focal length afterwards. This gave a FWHM pump angular intensity distribution of 0.16° and an intensity FWHM

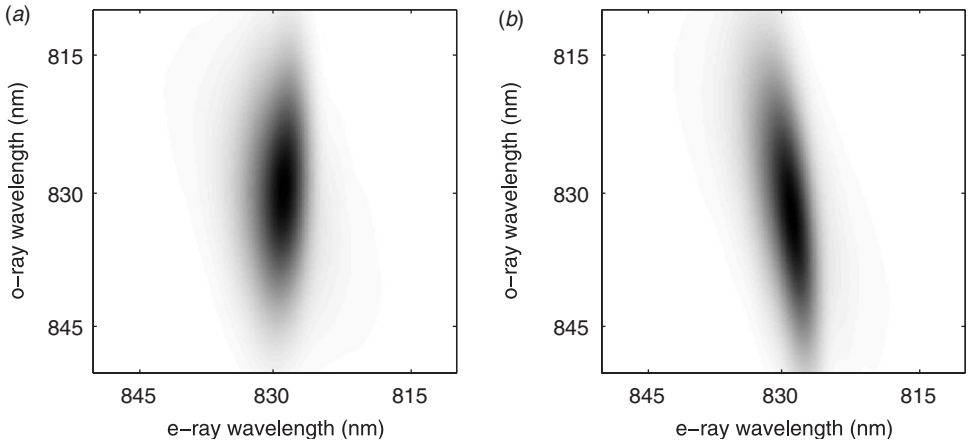

Figure 4. Numerically simulated joint spectra for the chosen experimental parameters. Positive spatial chirp (*a*) and negative spatial chirp (*b*).

pair collection angle of 0.30°. A more detailed description of the source setup is given elsewhere [14].

The predicted heralded purity from the amplitude distribution of a source using this set of parameters is 0.953 for positive spatial chirp but 0.839 if the spatial chirp is negative, as estimated using the numerical model outlined above. To test this prediction, two grating spectrometers were used to map the joint spectral intensity of the photon pairs [23,24]. Such a measurement determines the degree of spectral correlation, although it provides no information about the phase of the joint spectral amplitude and therefore the degree of temporal correlation remains unknown. With the e-ray downconverted photons coupled into one single-mode fibre and the o-rays into another, the exit faces of these two fibres replaced the entrance slits in two commercial grating spectrometers. The broadband o-rays were sent to an Andor Shamrock spectrometer and the narrower e-rays to a Jobin-Yvon Triax spectrometer. The gratings were chosen so that the angular dispersion of the e-ray photons would be about four times that of the o-ray photons and hence approximately equal to the inverse of the ratio of their spectral widths.

The output of each spectrometer was collected directly into a multimode fibre without any coupling optics. The core diameter of these fibres therefore defined the effective resolution of the spectrometers: larger diameter fibres gave increased count rates but reduced the resolution. The fibre tips were both mounted on motorized x and manual yz translation stages. The two manual translation axes allowed for accurate positioning of the fibre tips at both the correct height and longitudinal position in the focal planes of the spectrometers. The motorized x translation moved the fibres transversely across the focal planes and hence controlled the wavelength range that each fibre collected. On the output end of each fibre was a silicon avalanche photodiode (APD) for photon detection, connected to coincidence electronics. A diagram of the apparatus is shown in Figure 5.

In order to make the measurement in an efficient manner, it was important to match the resolution of the spectrometers to the count rates available. Although it is clearly advantageous to make a high-resolution measurement of the joint spectrum, it must be mapped in two dimensions and therefore the time taken to make the measurement goes up with the square of the number of steps. In addition, to make the resolution high a smaller diameter fibre is required. The number of photons collected is proportional to the square of the fibre core diameter, so the smaller the fibre the longer it is necessary to count for at each position to obtain an adequate number of events to ensure good statistics. Therefore the time required for each measurement is highly dependent on the fibre diameter and a compromise must be reached between count rates and resolution. For the count rates and resolution required here, 105 μm core fibres collecting the light from each spectrometer gave the best performance. The maximum resolution for each spectrometer with these fibres was found using classical light and a high-resolution optical spectrum analyser (OSA) on the multimode fibre outputs. The resolutions were 0.5 nm in the case of the Jobin-Yvon (e-ray) spectrometer and 2 nm for the Andor (o-ray). Both spectrometers were calibrated against the same factory-calibrated Ocean Optics USB2000 spectrometer.

With the downconversion coupled through the spectrometers, monitoring the coincidence rates between the two APDs while scanning independently the two stages allowed the joint spectral intensity to be

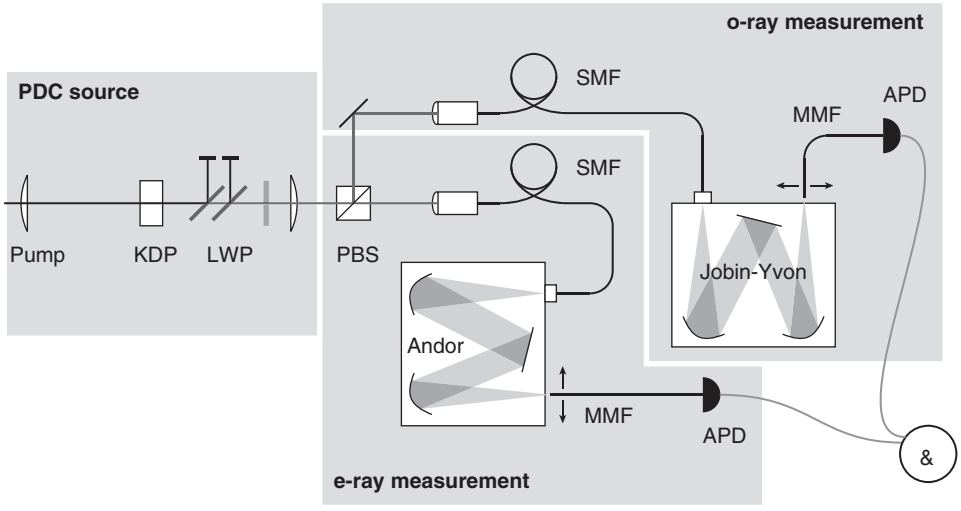

Figure 5. Apparatus for the joint spectral measurements. KDP = downconversion crystal, LWP = long-wave-pass filter, PBS = polarising beamsplitter, SMF = single-mode fibre, MMF = multimode fibre, APD = avalanche photodiode.

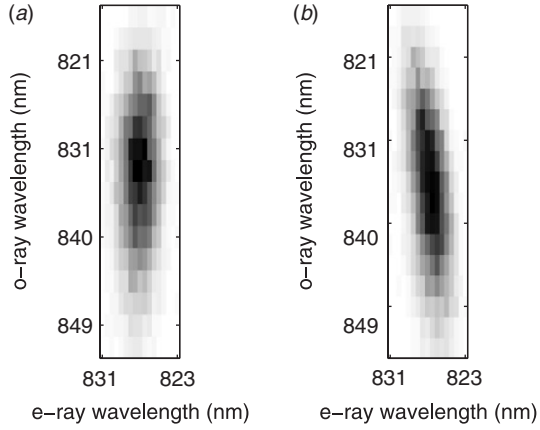

Figure 6. Joint spectra calculated from the numerical model for the experimental parameters with positive spatial chirp (*a*) and negative spatial chirp (*b*).

mapped. The fibres were scanned across the required wavelength range in a series of 16 steps, covering approximately 10 nm by 40 nm for e- and o-ray, respectively. The step sizes along each axis in this grid were therefore not equal; the e-ray was sampled at intervals of just over 0.5 nm, and the o-ray in steps slightly greater than 2 nm, close to the respective resolutions of the two spectrometers. Joint spectra were taken for both positive and negative spatial chirp by rotating the crystal 180° about the pump beam axis.

The experimental data are presented in Figure 6. For positive spatial chirp, the measured spectral intensity distribution is highly factorable; if flat spectral phase is assumed across the corresponding joint amplitude distribution, the associated purity is 0.979. On the other hand, for negative chirp the joint state is much less factorable, with an anticipated purity of 0.894. These figures compare favourably to those predicted at the beginning of this section.

An additional method of comparing the correlations present in the two measured spectra is to plot the e-ray wavelength at which the maximum count rate occurs at every o-ray position. This is most accurately done by fitting each data slice at constant o-ray wavelength with a Gaussian distribution in e-ray wavelength. The centres of these fits can then be plotted against the o-ray wavelength at which they were taken. The results are shown in Figure 7. For the measured spectra, in the case of the uncorrelated spectrum resulting from positive spatial chirp on the pump beam, it can be seen that the centre of the e-ray spectrum is almost constant over the entire o-ray spectrum. The fit line to these e-ray central wavelength points changes by only half a nanometre over 30 nm of

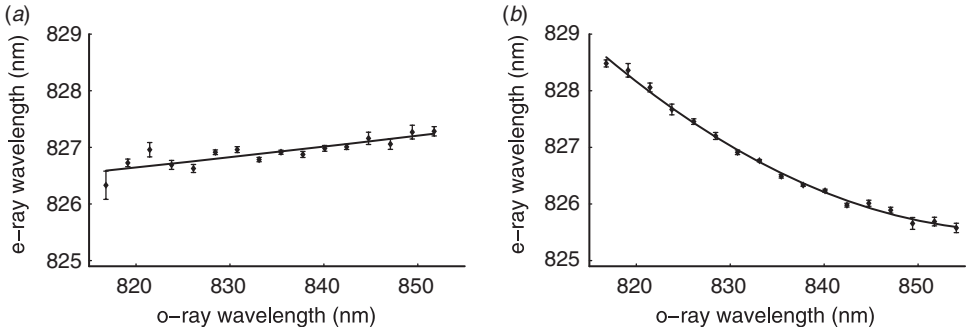

Figure 7. Plots of the central e-ray wavelengths of Gaussian fits to the coincidence data at constant o-ray wavelengths for the measured joint spectra. The correlation of e-ray wavelength on o-ray wavelength is shown for positive pump spatial chirp in (*a*) negative chirp in (*b*). The lines are quadratic fits to the data to guide the eye.

o-ray bandwidth, again demonstrating the factorable nature of this state. However, for negative spatial chirp, the e-ray centre wavelength is strongly anti-correlated with o-ray wavelength and exhibits a quadratic dependence.

The measurements of the joint spectra also allow estimates to be made of the bandwidths of the daughter photons. The marginal distribution of each photon is found by integrating over the frequency of the other. The total bandwidths of the o-rays were thus found to be 16.4 nm for positive chirp and 19.8 nm for negative chirp, and the bandwidth of the e-rays were approximately 3.5 nm in both cases.

7. Conclusion

Pure state single photon generation from PDC represents a significant step forward for photonic QIP. For the first time it has become possible to perform multi-source interference experiments with downconversion sources free of spectral filters. The original proposal for factorable state generation in KDP laid the theoretical foundations for the technique, but any successful experimental implementation must take into account additional effects not originally considered. The most important of these are the implications of focusing into the nonlinear crystal, and the associated effects of having a pump beam that is spatially inhomogeneous. Although this does make the situation more complex, these challenges should not been seen as disadvantages; their inclusion in a simple model demonstrates that one can end up with a state more factorable than would be possible with a collimated pump given the same crystal parameters.

A source exhibiting these characteristics has been demonstrated experimentally. By pumping KDP with the second harmonic of an ultrafast laser we have successfully generated type-II phasematched down-conversion with the group velocity of one daughter photon matched to that of the pump. As predicted, this produces photons whose joint spectra are factorable into a function of the signal photon frequency multiplied by a function of the idler. It has been proved that the joint spectral probability distribution of the photon pairs is factorable by directly measuring the joint spectral intensity with a pair of fibre coupled grating spectrometers. Heralding with one of these photons leaves the other in a pure state, something that can be seen by measuring the Hong–Ou–Mandel interference between the remaining single photons [25].

Acknowledgements

We thank Alfred B. U'Ren and Christine Silberhorn for insightful discussions, and Piotr Wasylczyk for assistance in the laboratory. This work was supported by the EPSRC (UK) through the QIP IRC (GR/S82716/01) and project EP/C013840/1, by the European Commission under the Integrated Project Qubit Applications (QAP) funded by the IST directorate as Contract Number 015848, and by the Royal Society.

References

[1] Hong, C.K.; Ou, Z.Y.; Mandel, L. *Phys. Rev. Lett.* **1987,** *59,* 2044–2046.

[2] Kwiat, P.G.; Mattle, K.; Weinfurter, H.; Zeilinger, A.; Sergienko, A.V.; Shih, Y. *Phys. Rev. Lett.* **1995,** *75,* 4337–4341.

[3] Ou, Z.Y.; Mandel, L. *Phys. Rev. Lett.* **1988,** *61,* 50–53.

[4] Pittman, T.B.; Franson, J.D. *Phys. Rev. Lett.* **2003,** *90,* 240401-1–4.

[5] O'Brien, J.L.; Pryde, G.J.; White, A.G.; Ralph, T.C.; Branning, D. *Nature.* **2003,** *426* (6964), 264–267.

[6] Chen, K.; Li, C.M.; Zhang, Q.; Chen, Y.A.; Goebel, A.; Chen, S.; Mair, A.; Pan, J.-W. *Phys. Rev. Lett.* **2007,** *99,* 120503.

[7] U'Ren, A.B.; Silberhorn, C.; Banaszek, K.; Walmsley, I.A.; Erdmann, R.; Grice, W.P.; Raymer, M.G *Laser Phys.* **2005,** *15,* 146–161.

[8] Riedmatten, H.D.; Marcikic, I.; Tittel, W.; Zbinden, H.; Gisin, N. *Phys. Rev. A* **2003,** *67,* 022301-1–5.

[9] Kaltenbaek, R.; Blauensteiner, B.; Zukowski, M.; Aspelmeyer, M.; Zeilinger, A. *Phys. Rev. Lett.* **2006,** *96,* 240502.
[10] Lu, C.Y.; Zhou, X.Q.; Guhne, O.; Gao, W.B.; Zhang, J.; Yuan, Z.S.; Goebel, A.; Yang, T.; Pan, J.-W. *Nature Physics.* **2007,** *3,* 91–95.
[11] Grice, W.P.; U'Ren, A.B.; Walmsley, I.A. *Phys. Rev. A* **2001,** *64,* 063815-1–7.
[12] U'Ren, A.B.; Erdmann, R.K.; de la Cruz-Gutierrez, M.; Walmsley, I.A. *Phys. Rev. Lett.* **2006,** *97,* 223602–223604.
[13] Garay-Palmett, K.; McGuinness, H.J.; Cohen, O.; Lundeen, J.S.; Rangel-Rojo, R.; Raymer, M.G.; McKinstrie, C.J.; Radic, S.; U'Ren, A.B.; Walmsley, I.A. *Opt. Express.* **2007,** *15,* 14870–14886.
[14] Mosley, P.J. Generation of Heralded Single Photons in Pure Quantum States. Ph.D. thesis, University of Oxford: Oxford, 2007.
[15] Walton, Z.D.; Sergienko, A.V.; Saleh, B.E.A.; Teich, M.C. *Phys. Rev. A* **2004,** *70,* 052317-1–5.
[16] U'Ren, A.B.; Mukamel, E.; Banaszek, K.; Walmsley, I.A. *Phil. Trans. R. Soc. A* **2003,** *361,* 1493–1506.
[17] Torres, J.P.; Macià, F.; Carrasco, S.; Torner, L. *Opt. Lett.* **2005,** *30,* 314–316.
[18] Carrasco, S.; Torres, J.P.; Torner, L.; Sergienko, A.; Saleh, B.E.A.; Teich, M.C. *Phys. Rev. A* **2004,** *70,* 043817-1–5.
[19] Valencia, A.; Cere, A.; Shi, X.; Molina-Terriza, G.; Torres, J.P. *Phys. Rev. Lett.* **2007,** *99,* 243601.
[20] Shi, X.; Valencia, A.; Hendrych, M.; Torres, J.P. *Opt. Lett.* **2008,** *33,* 875–877.
[21] Ljunggren, D.; Tengner, M. *Phys. Rev. A* **2005,** *72,* 062301-1–17.
[22] Wasylczyk, P.; U'Ren, A.B.; Mosley, P.J.; Lundeen, J.; Branderhorst, M.P.A.; Gorza, S.P.; Monmayrant, A.; Radunsky, A.; Walmsley, I.A. *J. Mod. Opt.* **2007,** *54,* 1939–1958.
[23] Kim, Y.H.; Grice, W.P. *Opt. Lett.* **2005,** *30,* 908–910.
[24] Poh, H.S.; Lum, C.Y.; Marcikic, I.; Lamas-Linares, A.; Kurtsiefer, C. *Phys. Rev. A* **2007,** *75,* 043816-1–8.
[25] Mosley, P.J.; Lundeen, J.S.; Smith, B.J.; Wasylczyk, P.; U'Ren, A.B.; Silberhorn, C.; Walmsley, I.A. *Phys. Rev. Lett.* **2008,** *100,* 133601.